ACS OMEGA

Open Access

http://pubs.acs.org/journal/acsodf

Article

Probing Antimicrobial Activity and Mechanism of Action of a Bile Acid-Derived Antibiotic

Colin C. Tang, Conor Pulliam, Alimi Abiodun, Adam Parris, Andrew Campbell, and Jie Li*

Cite This: *ACS Omega* 2025, 10, 1727−1734

Read Online

ACCESS | Metrics & More | Article Recommendations

ABSTRACT: Antibiotics have revolutionized medicine, saving countless lives since the introduction of penicillin. However, antimicrobial resistance has challenged their efficacy, prompting ongoing efforts to develop new antibiotics. This study explores the antimicrobial effects of a bile acid derivative, BA-3/4-Butyl. By analyzing the interactions of BA-3/4-Butyl with model bacterial (DOPC/DOPG) and mammalian (DOPC/cholesterol) membranes and by probing its mechanism of action against bacteria using a variety of assays and transmission electron microscopy (TEM) imaging, we reveal that BA-3/4-Butyl exerts its antimicrobial activity via membrane permeabilization. Our findings provide insights into how BA-3/4-Butyl compromises bacterial membranes without causing toxicity in its mammalian counterparts. This study advances the understanding of BA-3/4-Butyl's antimicrobial activity and potential mechanisms of action, ultimately aiding the development of similar novel therapeutic agents to help combat antimicrobial resistance.

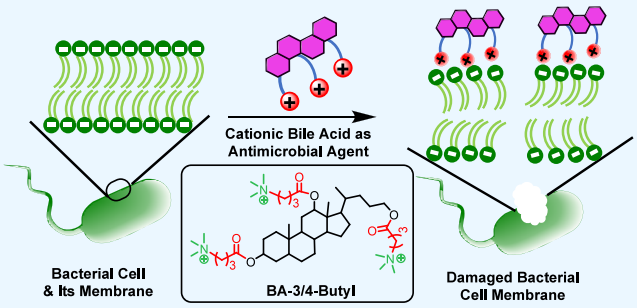

1. INTRODUCTION

Antibiotics have saved millions of lives since the initial discovery of penicillin in the 1930s.[1,2] Since then, numerous antibiotics have been developed to treat a variety of bacterial infections. However, the rising prevalence of multidrug-resistant bacteria in healthcare settings has necessitated the discovery of new antibiotics with potent biological activities and novel mechanisms of action that can evade bacterial resistance.[3] Discovering new antimicrobials and understanding their mechanisms of action is thus important in reducing the occurrence of antibiotic resistance. By elucidating how antibiotics interact with bacterial cells, more effective therapeutic agents can be designed. One prevalent strategy in antibiotic development involves targeting and disrupting bacterial plasma and outer membrane components.[4,5] Compromising these membranes can effectively incapacitate bacteria and prevent infections.[6,7]

Among the various classes of compounds investigated for their antimicrobial properties, bile acids have garnered attention due to their diverse biological functions.[8−10] Recently, synthetic derivatives of bile acids have demonstrated promising antimicrobial activity against a variety of different bacteria.[11,12] One such bile acid-derived compound, BA-3/4-Butyl, has demonstrated significant efficacy against numerous Gram-negative bacteria.[13,14] BA-3/4-Butyl consists of a tetracyclic hydrocarbon skeleton (bile acid backbone) with three 4-carbon alkyl spacers connected via an ester bond and ending in a quaternary amine functional group (Figure 1). These quaternary amines are positioned on the bile acid

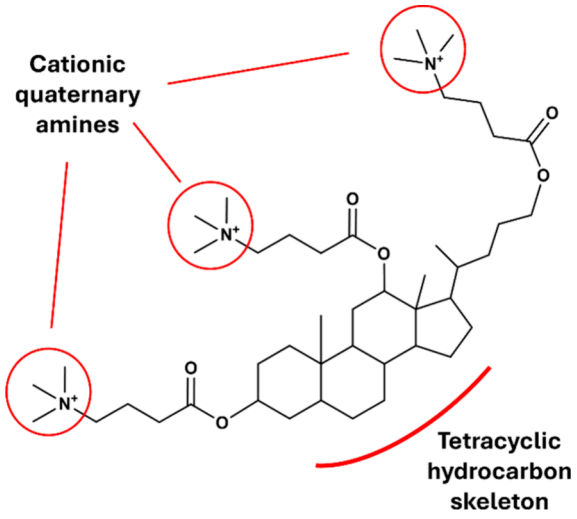

Figure 1. Structure of BA-3/4-Butyl.

Received: October 27, 2024
Revised: December 4, 2024
Accepted: December 13, 2024
Published: December 23, 2024

backbone to enable them to cluster to one side of the molecule, constituting the hydrophilic portion of the molecule, while the hydrophobic backbone remains on the opposite side of the molecule. This functional group organization imparts amphiphilic properties to BA-3/4-Butyl, which we hypothesize contributes to its antimicrobial activity. However, the precise mechanism through which BA-3/4-Butyl exerts its antimicrobial activity is unknown and requires further investigation. This study aims to understand the molecular interactions between biological membranes and BA-3/4-Butyl *in vitro* using model membranes, while also investigating the antimicrobial activity of BA-3/4-Butyl against *B. subtilis* and *E. coli*. This study ultimately provides new insights into the mechanism of action of BA-3/4-Butyl, laying a foundation for the study of other bile acid derivatives with potential for development as therapeutic agents.

2. RESULTS

2.1. Preparation of Membrane-Mimicking Lipid Vesicles. To begin probing the mechanism of action of BA-3/4-Butyl, we prepared vesicles mimicking either bacterial or mammalian membranes using 1,2-dioleoyl-*sn*-glycero-3-phosphocholine (DOPC), 1,2-dioleyl-phosphatidyl-glycerol (DOPG), and cholesterol. As shown in Figure 2, DOPC is

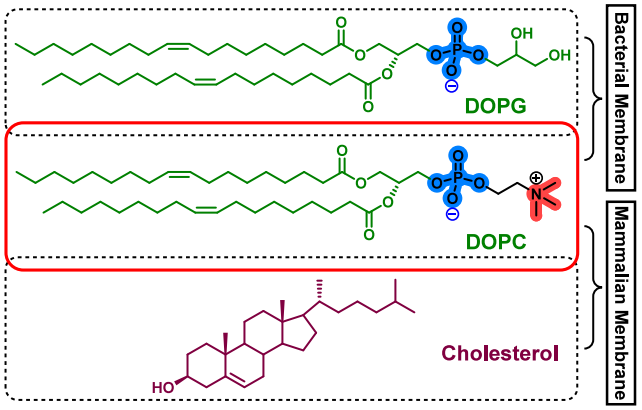

Figure 2. Components used to construct bacterial and mammalian membrane mimics.

zwitterionic and therefore net neutral, DOPG carries a net negative charge, and cholesterol is uncharged.[15] Based on previous reports, we combined DOPC and DOPG in a 70/30 ratio to prepare bacterial membrane mimics and combined DOPC and cholesterol in a 70/30 ratio to prepare mammalian membrane mimics. A sonication-freeze−thaw process was performed five times to produce a clear solution. These ratios of DOPC, DOPG, and cholesterol were previously demonstrated by multiple groups to be effective in creating bacterial and mammalian membrane mimics.[16−20]

After constructing the membrane-mimicking vesicles, we characterized them using dynamic light scattering (Table 1). DOPC/DOPG vesicles (bacterial membrane-mimicking) have an average diameter of 234 nm with a highly negative Zeta potential of −32.5 mV, the latter of which is comparable to previously reported Zeta potentials.[18] DOPC/cholesterol vesicles (mammalian membrane-mimicking) have an average diameter of 136.7 nm and a Zeta potential of −4.5 mV, much closer to neutral in Zeta potential compared to bacterial membrane mimcs.[17] These results further indicated the successful preparation of lipid vesicles.

Table 1. Size and Zeta Potential of Membrane-Mimicking Lipid Vesicles via Dynamic Light Scattering

Vesicle Composition	Average Diameter	Zeta Potential
DOPC/DOPG	234.0 ± 64.5 nm	−32.5 ± 16.0 mV
DOPC/cholesterol	136.7 ± 1.3 nm	−4.5 ± 1.4 mV

2.2. Dye Leakage Analysis. Given the nature of all-lipid cell membranes that consist of lipophilic alkyl tails and hydrophilic heads, there is potential for amphiphilic compounds to interact with the model lipid vesicles. However, due to the differential potentials of our bacterial and mammalian membrane mimics, we hypothesized that cationic amphiphilic compounds such as BA-3/4-Butyl may selectively interact with the more negatively charged bacterial membranes, as opposed to the near-neutral mammalian membranes, to exert biological activity. Thus, we constructed similar membrane mimics as previously, but with the dye calcein added during the construction process, resulting in membranes with calcein trapped inside the lipid bilayer. We hypothesized that if BA-3/4-Butyl interacted with and damaged the membrane, calcein would be released from the membrane, which could be measured by fluorescence (Figure 3).

To determine the ability of BA-3/4-Butyl to damage the membrane, we first determined the baseline fluorescence of the bacterial and mammalian vesicles with trapped calcein without any treatment. As expected, no significant increase in fluorescence was observed in the absence of BA-3/4-Butyl. We then added Triton X-100, a known membrane-permeabilizing agent, to the vesicles and measured the fluorescence intensity over time as a positive control for comparison to BA-3/4-Butyl. Using these fluorescence measurements, we could determine the leakage percentage of the membranes following addition of BA-3/4-Butyl using the expression $L = 100 \times [(I-I_0)/(I_{TX}-I_0)]$, where L is the leakage percentage, I is the fluorescence intensity of the vesicles with BA-3/4-Butyl added, I_0 is the baseline fluorescence intensity of the vesicles alone, and I_{TX} is the fluorescence intensity of the vesicles with Triton X-100 added.

We synthesized BA-3/4-Butyl following previously reported protocols[14] and used it for the dye leakage assay and subsequent experiments. The dye leakage experiment was first carried out with the bacterial membrane-mimicking vesicles. Fluorescence measurements of the dye-containing membranes were taken after adding varying concentrations of BA-3/4-Butyl (Figure 4A). These measurements showed a dose-dependent increase in fluorescence and therefore leakage, suggesting the ability of BA-3/4-Butyl to damage the membrane and allow calcein release. We then studied the leakage effect of BA-3/4-Butyl against the mammalian membrane-mimicking vesicles. In contrast to the bacterial mimic vesicles, the mammalian mimic vesicles exhibited minimal membrane leakage when exposed to BA-3/4-Butyl. The average leakage values at varying concentrations of BA-3/4-Butyl were then plotted for both types of vesicles, further emphasizing the selectivity of BA-3/4-Butyl for bacterial membrane mimics over mammalian membrane mimics (Figure 4B). Our findings that BA-3/4-Butyl showed minimal membrane-damaging effects against mammalian membrane mimics is in agreement with a previous report showing that BA-3/4-Butyl has low hemolytic activity.[13] These results confirmed that BA-3/4-Butyl caused significant damage to

https://doi.org/10.1021/acsomega.4c09804
ACS Omega 2025, 10, 1727−1734

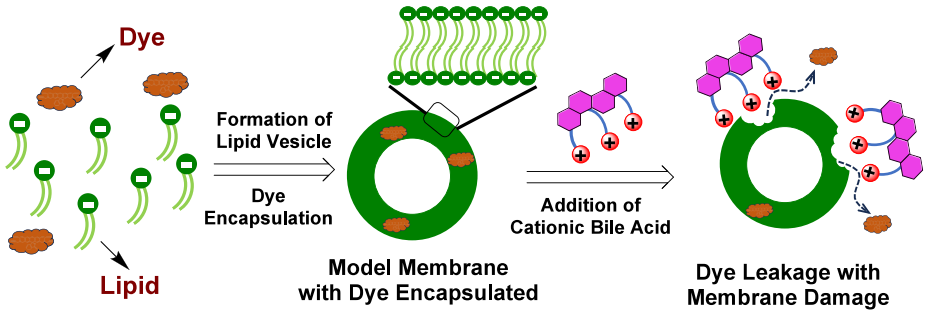

Figure 3. Illustration of dye leakage of bacterial membrane-mimicking lipid vesicles exposed to BA-3/4-Butyl.

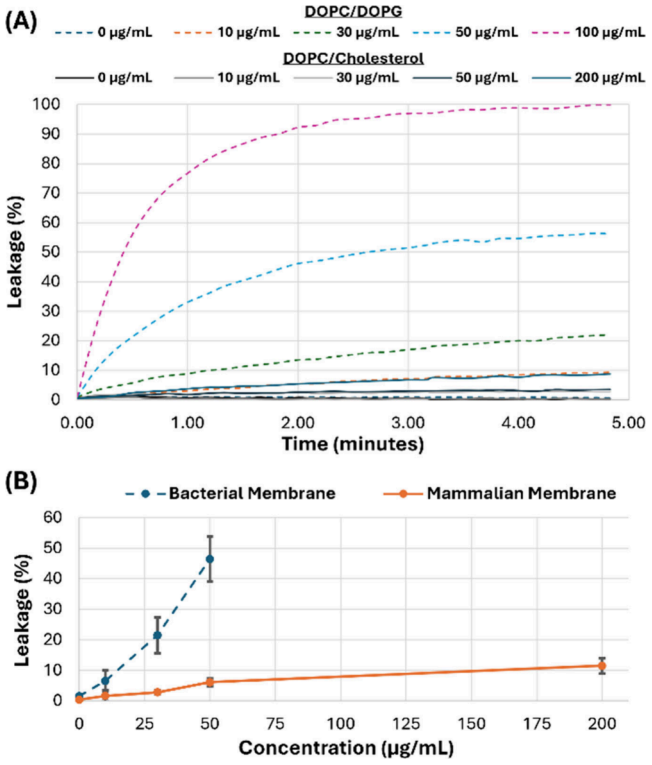

Figure 4. (A) Dye leakage profiles of DOPC/DOPG vesicles (dashed lines, mimicking bacterial membranes) and DOPC/cholesterol vesicles (solid lines, mimicking mammalian membranes) with different concentrations of BA-3/4-Butyl. (B) Dye leakage comparison of BA-3/4-Butyl against model bacterial vs mammalian membranes.

the model bacterial membrane, while it had a minimal impact on the mammalian membrane, further supporting its safety profile and its potential as an antimicrobial therapeutic.

2.3. Antimicrobial Activity and MIC Determination.

The dye leakage assay suggested that BA-3/4-Butyl has the potential to compromise bacterial cell membranes. Thus, we moved to an live-cell model to study BA-3/4-Butyl's antimicrobial activity further. We used *Bacillus subtilis* Ehrenberg (Cohn) 6051 (*B. subtilis* 6051) as a representative to test the antimicrobial activity of BA-3/4-Butyl against Gram-positive species and *Escherichia coli* K-12 with the efflux pump component *tolC* deleted (*E. coli* Δ*tolC*) as a representative to test the activity of BA-3/4-Butyl against Gram-negative species. We performed a soft agar disk diffusion assay, using soft agar inoculated with one of the test strains and paper disks containing varying amounts of BA-3/4-Butyl dissolved in 2% dimethyl sulfoxide (DMSO). We added a solution of only 2% DMSO to another disk as a negative control and the antibiotics chloramphenicol and apramycin to two other disks as positive controls. We applied either 50 μg or 25 μg of BA-3/4-Butyl to test the dose dependence of its antimicrobial activity. We then observed the zones of inhibition, which revealed a dose-dependent increase in the sizes of the zones with increasing amount of BA-3/4-Butyl (Table 2), demonstrating the

Table 2. Inhibition Zone Sizes in the Disk Diffusion Assay Using Varying Concentrations of BA-3/4-Butyl against *B. subtilis* 6051 and *E. coli* Δ*tolC*

Compound	Diameter of Zone of Inhibition for *B. subtilis* 6051 (cm)	Diameter of Zone of Inhibition for *E. coli* Δ*tolC* (cm)
50 μg BA-3/4 -Butyl	3.3	1.7
50 μg chloramphenicol	4.0	3.4
50 μg apramycin	2.4	2.1
25 μg BA-3/4 -Butyl	2.5	1.4
25 μg chloramphenicol	3.4	2.8
25 μg apramycin	1.9	1.7

significant antimicrobial activity of BA-3/4-Butyl against both *B. subtilis* 6051 and *E. coli* Δ*tolC*. Intriguingly, BA-3/4-Butyl seemed to be significantly more effective in inhibiting the growth of *B. subtilis* 6051 compared to its inhibition of *E. coli* Δ*tolC*, as evidenced by the larger zones of inhibition measured for *B. subtilis* 6051 for both doses tested (Figure 5).

After qualitatively confirming the antimicrobial activity of BA-3/4-Butyl, we sought to determine its minimum inhibitory concentration (MIC) against *B. subtilis* 6051 and *E. coli* Δ*tolC*. Toward this goal, we used a 96-well dilution assay where we added 2-fold dilutions of BA-3/4-Butyl, beginning at 64 μg/mL and ending at 0.5 μg/mL, to LB media inoculated with *B. subtilis* 6051 or *E. coli* Δ*tolC* (Figure 5). We additionally included a well with no BA-3/4-Butyl added as a negative control. From this dilution assay, we determined the MIC of BA-3/4-Butyl against *B. subtilis* 6051 to be 4 μg/mL and against *E. coli* Δ*tolC* to be 16 μg/mL. These results were consistent with the observation in the disk diffusion assay that BA-3/4-Butyl formed larger zones of inhibition against *B. subtilis* 6051 than it did against *E. coli* Δ*tolC*. The different efficacy of BA-3/4-Butyl against Gram-positive and Gram-negative bacteria potentially suggests the target of BA-3/4-Butyl. It is likely that BA-3/4-Butyl targets a component of the plasma membrane, as this target would be accessible by BA-3/4-Butyl for Gram-positive species, but less accessible against

https://doi.org/10.1021/acsomega.4c09804
ACS Omega 2025, 10, 1727−1734

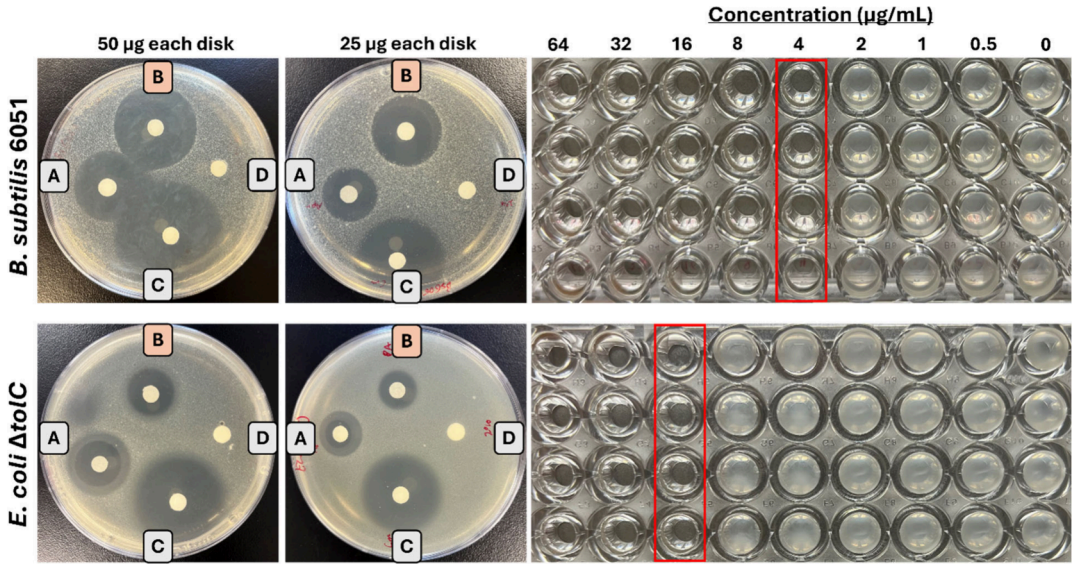

Figure 5. Antimicrobial activity of BA-3/4-Butyl against *B. subtilis 6051* and *E. coli* Δ*tolC*. Disk diffusion assay plates are shown on the left. The letter next to each disk represents what solution was applied to the disk. The labels represent the following solutions applied: A - Apramycin; B - BA-3/4-Butyl; C - Chloramphenicol; D - 2% DMSO in water. The amount of compound added to each disk is shown above the plates; for the "D" disks, 5 μL of 2% DMSO was added to each disk. On the right, the MIC-determining dilution assay is shown, demonstrating the MIC of BA-3/4-Butyl of 4 μg/mL against *B. subtilis* 6051 and 16 μg/mL against *E. coli* μ*tolC*.

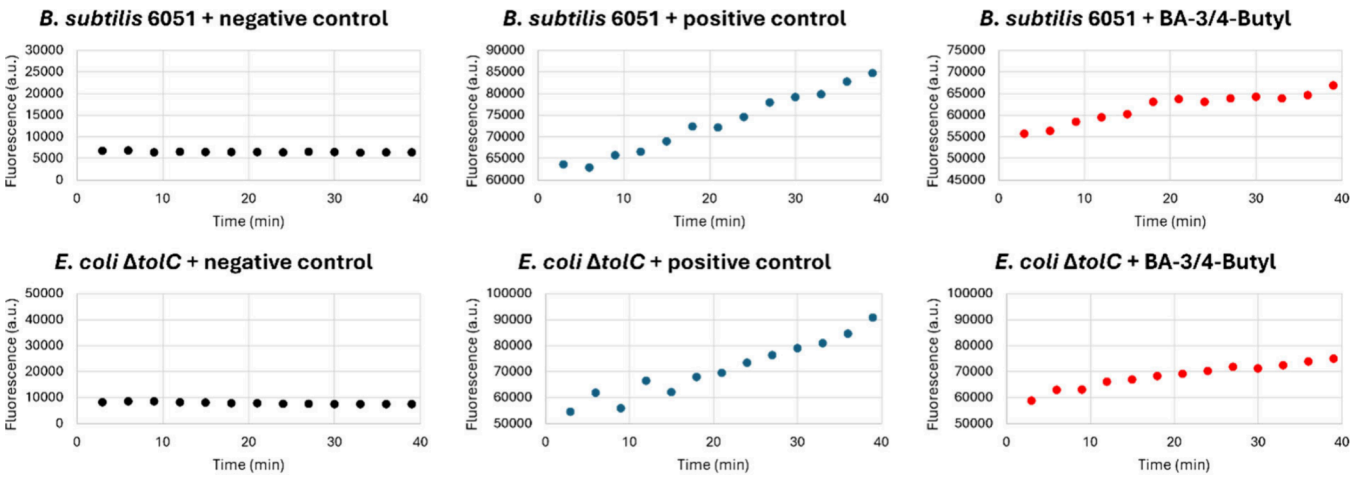

Figure 6. BA-3/4-Butyl exerts antimicrobial activity via membrane permeabilization. The results of the membrane permeability assay are shown, demonstrating no increase in fluorescence in the negative control groups, but increased fluorescence in the groups treated with BA-3/4-Butyl or the positive control Triton X-100. In the *B. subtilis* 6051 test group, 0.25x MIC of BA-3/4-Butyl (1 μg/mL) was used; in the *E. coli* Δ*tolC* test group, 1x MIC of BA-3/4-Butyl (16 μg/mL) was used.

Gram-negative species due to the presence of the outer membrane limiting the ability of BA-3/4-Butyl to reach the membrane.

2.4. Probing Mechanism of Action. After confirming the biological activity of BA-3/4-Butyl and noting its particular effectiveness against Gram-positive bacteria, we sought to investigate its mechanism of action. Based on the results from our *in vitro* dye leakage assay with bacterial and mammalian membrane mimics, which suggested that BA-3/4-Butyl interacts with bacterial membrane components, and our antimicrobial activity assays against *B. subtilis* 6051 and *E. coli* Δ*tolC* strains, we hypothesized that BA-3/4-Butyl may interact with the plasma membrane to exert its antimicrobial activity. Thus, we first performed a membrane permeability assay[21] using SYTOX Green, a membrane-impermeable dye that has amplified fluorescence when it binds intracellular DNA. If BA-3/4-Butyl interacts with and permeabilizes the bacterial plasma membrane, SYTOX Green should be able to enter the bacterial cells and bind to chromosomal DNA, resulting in increased fluorescence that can be monitored over time. We performed this assay in a 96-well plate using a well with SYTOX Green and *B. subtilis* 6051 or *E. coli* Δ*tolC*, but no BA-3/4-Butyl, as a negative control. As a positive control, we used SYTOX Green, Triton X-100, and *B. subtilis* 6051 or *E. coli* Δ*tolC*. Our test groups consisted of SYTOX Green, *B. subtilis* 6051 or *E. coli* Δ*tolC*, and BA-3/4-Butyl at varying concentrations. After adding the reagents to their corresponding wells, fluorescence measurements were taken every 3 min for a total of 39 min. Our measurements expectedly showed that the fluorescence of our negative controls did not increase significantly over time, while the fluorescence of our positive controls did increase significantly (Figure 6), thus verifying this

https://doi.org/10.1021/acsomega.4c09804
ACS Omega 2025, 10, 1727−1734

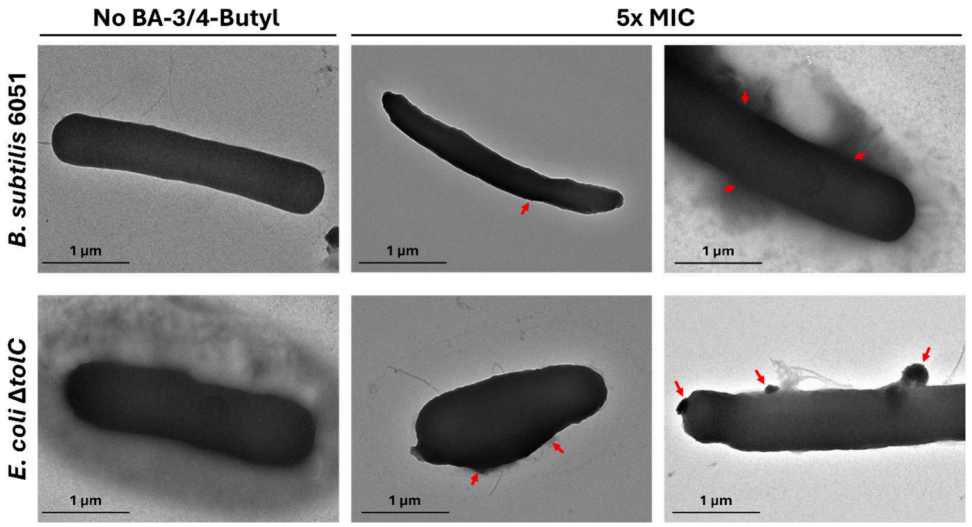

Figure 7. TEM imaging of *B. subtilis* 6051 and *E. coli* Δ*tolC* alone or in the presence of 5x MIC of BA-3/4-Butyl. In the untreated groups, normal rod-shaped cellular morphology is observed for both strains with no visible breaks in the membrane. In the 5x MIC treatment groups, alterations in cellular morphology are observed for *B. subtilis* 6051 as indicated by an elongated and irregular rod shape (top, middle), as well as for *E. coli* Δ*tolC* as indicated by a compressed and irregular rod shape (bottom, middle). Furthermore, several regions of membrane damage are observed in the 5x MIC-treated cells, including distinct bulging and breaks in the membrane. These regions of membrane damage are indicated by a red arrow.

method in determining the membrane-permeabilizing effects. In our test groups, we observed significant fluorescence increases in the *B. subtilis* 6051 test group after adding BA-3/4-Butyl, as well as fluorescence increases in the *E. coli* Δ*tolC* test group. Intriguingly, this membrane permeabilizing effect occurred at only 0.25x MIC value for *B. subtilis* 6051 (1 μg/mL), while it occurred at the MIC value for *E. coli* Δ*tolC* (16 μg/mL). These results suggest that the bacterial membrane is indeed impacted by BA-3/4-Butyl. The plasma membrane as a potential target for BA-3/4-Butyl is additionally supported by our *in vitro* dye leakage assay suggesting that the specificity of BA-3/4-Butyl depends on the net charge of the membrane it is interacting with, as it has been previously reported that the bacterial plasma membrane has a more negative net charge than the outer membrane.[22] Thus, it is logical that BA-3/4-Butyl would selectively interact with the more negatively charged plasma membrane over the outer membrane. Overall, these data suggested that BA-3/4-Butyl indeed exerts its biological activity via interaction with and permeabilization of the bacterial plasma membrane.

Following our membrane permeability assay suggesting the potential of BA-3/4-Butyl to damage the bacterial membrane, we sought to further confirm this potential mechanism of action via TEM imaging. We imaged *B. subtilis* 6051 and *E. coli* Δ*tolC* alone or in the presence of BA-3/4-Butyl at either 1x or 5x the respective MIC for each strain. The 1x MIC- and 5x MIC-treated groups showed similar results; thus, only the 5x MIC group images are shown to emphasize the altered morphology and membrane damage exhibited by the cells when exposed to BA-3/4-Butyl. Our results demonstrated that the untreated groups exhibited normal cellular morphology and membrane integrity, characterized by a uniform rod shape and no visible breaks in the membrane. In the 5x MIC-treated groups, however, significant membrane disruption was observed, as indicated by an elongated or compressed morphology compared to the untreated groups, as well as bulging and breaks in the membrane (Figure 7). Altogether, the results of our membrane permeability assay combined with our TEM imaging suggested that BA-3/4-Butyl exerts its antimicrobial activity through membrane damage. However, further studies should be performed to determine if BA-3/4-Butyl acts solely on the plasma membrane or if it is able to interact with and disrupt the outer membrane of Gram-negative bacteria.

3. DISCUSSION

In summary, we investigated the antimicrobial activity of a bile-acid derived antibiotic, BA-3/4-Butyl, against both Gram-positive and -negative bacteria, as well as the potential mechanism of action of this antibiotic. Initially using bacterial membrane-mimicking DOPC/DOPG vesicles and mammalian membrane-mimicking DOPC/cholesterol vesicles, we suggested the ability of BA-3/4-Butyl to target and disrupt the negatively charged bacterial membrane while causing minimal disruption to the mammalian membrane using a calcein-based dye leakage assay. Our results were further supported by earlier reports of the low hemolytic and cytotoxic activities of BA-3/4-Butyl,[13] indicating its potential as a therapeutic agent with a good safety profile. We further investigated the antimicrobial activity of BA-3/4-Butyl using disk diffusion and 96-well plate broth dilution assays, allowing us to determine dose dependence of the antimicrobial activity of BA-3/4-Butyl and the MIC of BA-3/4-Butyl against the representative Gram-positive species *B. subtilis* 6051 (4 μg/mL) and the representative Gram-negative species *E. coli* Δ*tolC* (16 μg/mL). These assays also suggested that BA-3/4-Butyl exerts antimicrobial activity by damaging lipid membranes. We then provided additional evidence supporting the ability of BA-3/4-Butyl to interact with and permeabilize bacterial membranes using a SYTOX Green-based membrane permeabilization assay, and finally confirmed this membrane-acting activity via TEM imaging of untreated and treated bacterial cells. Overall, this study provides further insights into the molecular actions of bile acid-derived antibiotics, which will aid the development of similar antibiotics to help combat the rising prevalence of antimicrobial resistance.

https://doi.org/10.1021/acsomega.4c09804
ACS Omega 2025, 10, 1727−1734

4. MATERIALS AND METHODS

General Materials. DOPC and DOPG sodium salt chloroform solutions and cholesterol were purchased from Avanti Polar Lipids. Calcein dye in powdered form was purchased from Cayman Chemical Company. Triton X-100, sodium chloride, and sodium hydroxide were purchased from Sigma-Aldrich. Chloramphenicol, apramycin, and Cytiva Sephadex G-25 Superfine were purchased from Fisher Scientific. BA-3/4-Butyl was previously synthesized and supplied by the University of South Carolina. *Bacillus subtilis* Ehrenberg (Cohn) 6051 and LB nutrient agar were purchased from ATCC. *E. coli* Δ*tolC* strain was a gift from the Bradley Moore lab at University of California San Diego. A SpectraMax M5Multimode Microplate Reader from Molecular Devices was used to monitor fluorescence.

Synthesis of BA-3/4-Butyl. A previously reported protocol was used for the synthesis of BA-3/4-Butyl.[14] Deoxycholic acid was used as a starting material and was treated with $LiAlH_4$ in dry THF to yield deoxycholic alcohol. This was then treated with 4-bromobutyryl chloride in 4-dimethylaminopyridine (DMAP) and triethylamine (TEA) to yield deoxycholic ester. This was then treated with trimethylamine in THF, ultimately yielding BA-3/4-Butyl. Correct product was confirmed by NMR analysis.

Preparation of Lipid Vesicles. Two buffer solutions were first prepared, each using disodium hydrogen phosphate. Buffer A was made using 284 mg Na_2HPO_4 and 200 mL H_2O. Buffer B (PBS buffer) was prepared using 100 mL of Buffer A and 526 mg of NaCl. To prepare the lipid vesicles, a 7:3 ratio of DOPC and DOPG was used, both in chloroform solution. 275 μL DOPC and 120 μL DOPG were mixed into a round-bottom flask. Following a reported procedure,[18] the solution was vacuum-dried for 2 h until it changed from clear liquid to white coating/stains. Next, the lipid solution was added with a calcein phosphate buffer, which was prepared by mixing 249 mg calcein, 10 mL Buffer A, and 4.80 mL 0.4% (w/v) aqueous NaOH solution. After 1 h stirring, a process of sonication (5 min) and freeze thaw in liquid nitrogen was done five times to allow for a color change from white to clear. Once this process was completed, the solution was added to a Sephadex G-25 buret column and eluted with Buffer B. Eight vesicle solutions of equal volume (2 mL) were collected from the elution. The second solution eluted was chosen and a 100-fold dilution was made by successively diluting with Buffer B. This 100-fold dilution was used for subsequent dye leakage assays. Comparatively, vesicles of DOPC and cholesterol at a ratio of 7:3 were also prepared, using the above-mentioned process for the preparation of DOPC/DOPG vesicles.

Dye Leakage Assay. For fluorescence measurements of the calcein-containing lipid vesicles, 1.47 mL of PBS buffer and 15 μL vesicle solution were first mixed in a glass cuvette. The cuvette was placed into the spectrometer for 1 min for calibration of baseline fluorescence intensity measurements (I_0). Then, 15 μL of Triton X-100 was added to the cuvette solution and measurements were recorded for 5 min to determine the value of I_{TX}. For the test group fluorescence measurements, 1.47 mL of PBS buffer, 15 μL vesicle solution, and 15 μL of BA-3/4-Butyl of varying concentrations was added to a glass cuvette and fluorescence measurements were recorded for 5 min to determine the value of I. This procedure was repeated 30 times for each test group. Findings were reported in leakage intensity, L (%).

Disk Diffusion Assay. Overnight cultures of *B. subtilis* 6051 and *E. coli* Δ*tolC*, grown at 30 and 37 °C, respectively, were diluted 2500-fold into 10 mL of LB broth for each strain. Subsequently, 10 mL of molten LB agar (0.8% w/v) was poured into a 50 mL Falcon tube and allowed to cool for several minutes. After cooling, the 10 mL of each of the 2500-fold diluted strains was then added to the 10 mL of molten LB agar for a 5000-fold total dilution in soft LB agar (0.4% w/v) and poured to create a soft agar plate inoculated with respective strains. After the plates cooled and solidified, sterile paper disks were then added to the plates. To each disk was added a solution of 2% DMSO, apramycin, chloramphenicol, or varying concentrations of BA-3/4-Butyl, where DMSO acted as a negative control while apramycin and chloramphenicol acted as positive controls. After adding respective treatments, the plates were incubated overnight at 30 or 37 °C for *B. subtilis* 6051 or *E. coli* Δ*tolC*, respectively. The following day, the diameters of the zones of inhibition around each disk of each plate were measured and tabulated to compare antibiotic activity.

96-Well Plate Dilution Assay. Overnight cultures of *B. subtilis* 6051 and *E. coli* Δ*tolC* were diluted 5000-fold into fresh LB broth. Then, 45 μL of these dilutions were added to their respective rows in a 96-well plate. Serial dilutions of BA-3/4-Butyl, beginning at 640 μg/mL and ending at 5 μg/mL, were then prepared in water, and 5 μL of each of these solutions was added to their respective wells (10x dilution), resulting in bacterial suspensions containing serially diluted BA-3/4-Butyl across the plate, beginning at 64 μg/mL and ending at 0.5 μg/mL. As a control without BA-3/4-Butyl, 50 μL of the 500-fold bacterial dilution in LB broth was added to one extra column of the 96-well plate. Furthermore, 50 μL of LB (not inoculated) was added to the remaining wells on the edges of the plate to reduce evaporation effects. The plate was then covered and wrapped in parafilm to prevent evaporation and subsequently incubated at 37 °C overnight. The next day, the plate was visually examined for turbidity to determine MIC values for each strain.

Membrane Permeability Assay. Overnight cultures of *B. subtilis* 6051 and *E. coli* Δ*tolC* were grown at 30 and 37 °C, respectively, with shaking. The following morning, each of these cultures was diluted 100-fold into 10 mL LB and incubated until OD_{600} reached 0.5−0.6. The cells were then centrifuged at 1000 × g for 10 min at 15 °C. The supernatant was poured off and the pellet was washed with 5 mL of sterile 5 mM HEPES by resuspension and centrifuged again. The supernatant was poured off and the pellet was resuspended in 5 mL of sterile 5 mM HEPES. To a black-bottom 96-well plate, 99.4 μL of each cell suspension was added to their corresponding wells. For control wells with no cells, 99.4 μL of sterile phosphate-buffered saline (PBS) was added instead. To every well, 0.1 μL of a 5 mM stock solution of SYTOX Green was added and mixed. Baseline fluorescence measurements were then collected using a Synergy H1 hybrid plate reader at an excitation wavelength of 488 nm and emission wavelength of 523 nm. Baseline measurements were taken every 30 s until the signal stabilized. Following baseline measurement, 0.5 μL of 200x stock solutions of the treatments (BA-3/4-Butyl or Triton X-100) were added to their respective wells. Following addition of treatments, fluorescence was measured every 3 min for 20 cycles.

TEM Imaging. *B. subtilis* 6051 and *E. coli* Δ*tolC* were cultured overnight in LB broth at 30 and 37 °C, respectively.

https://doi.org/10.1021/acsomega.4c09804
ACS Omega 2025, 10, 1727−1734

The following morning, the OD_{600} of the cultures was measured using an Eppendorf BioSpectrometer Kinetic and were subsequently diluted to OD_{600} = 0.5 in 500 μL LB in six 1.5 mL microcentrifuge tubes (3 tubes for *B. subtilis* 6051 and 3 for *E. coli* Δ*tolC*). Two of the tubes from each strain were left untreated, two were treated with a final concentration of 1x MIC for the respective strain (4 μg/mL for *B. subtilis* 6051 and 16 μg/mL for *E. coli* Δ*tolC*), and the remaining two were treated with 5x MIC for the respective strain (20 μg/mL for *B. subtilis* 6051 and 80 μg/mL for *E. coli* Δ*tolC*). Each tube was mixed well and then allowed to incubate at room temperature for 30 min before further processing. After incubation, the untreated and treated cells were centrifuged at 2500 xg for 5 min. The supernatant was removed and the cells were resuspended in 2.5% glutaraldehyde in 0.1 M sodium cacodylate buffer and subsequently incubated at 4 °C for 15 min for fixation. After incubation, the cells were pelleted at 2500 xg for 5 min and subsequently resuspended in aqueous 2% OsO_4 and allowed to incubate at 4 °C for 15 min for postfixation and staining. Lastly, the cells were pelleted at 2500 xg and resuspended in 0.1 M sodium cacodylate buffer to remove excess OSO_4. A 10 μL drop of each processed cell suspension was then added to its respective 300 mesh copper-Formvar TEM grid (FCF300H−Cu−SC, 10 nm Formvar, 20−30 nm carbon; Electron Microscopy Sciences) and allowed to air-dry for 1 h. Excess liquid was removed from the grids with filter paper prior to imaging. TEM imaging was performed with a Hitachi HT7800 TEM operating at 100 kV.

AUTHOR INFORMATION

Corresponding Author

Jie Li − *Department of Chemistry and Biochemistry, University of South Carolina, Columbia, South Carolina 29208, United States;* orcid.org/0000-0001-7977-6749; Email: LI439@mailbox.sc.edu

Authors

Colin C. Tang − *Department of Chemistry and Biochemistry, University of South Carolina, Columbia, South Carolina 29208, United States*

Conor Pulliam − *Department of Chemistry and Biochemistry, University of South Carolina, Columbia, South Carolina 29208, United States;* orcid.org/0009-0009-1512-7956

Alimi Abiodun − *Department of Chemistry and Biochemistry, University of South Carolina, Columbia, South Carolina 29208, United States*

Adam Parris − *Department of Chemistry and Biochemistry, University of South Carolina, Columbia, South Carolina 29208, United States*

Andrew Campbell − *Department of Chemistry and Biochemistry, University of South Carolina, Columbia, South Carolina 29208, United States*

Complete contact information is available at: https://pubs.acs.org/10.1021/acsomega.4c09804

Author Contributions

Colin Tang: Conceptualization, investigation, data curation, writing. **Conor Pulliam**: Investigation, supervision, data curation, writing. **Alimi Abiodun**: Supervision, data curation. **Adam Parris**: Data curation. **Andrew Campbell**: Investigation, data curation. **Jie Li**: Methodology, supervision, reviewing and editing.

Notes

The authors declare no competing financial interest.

ACKNOWLEDGMENTS

We would like to acknowledge Dr. JiHyeon Hwang at the University of South Carolina for initial assistance in the preparation of DOPC/DOPG vesicles and Dr. Silvia Atim for assistance and research encouragement. This work is part of a Discovery Magnet Science Project from Spring Valley High School (Columbia, SC). C. Tang acknowledges the Magnet Programs at Spring Valley High School and thanks Mrs. Heather Alexander, Dr. Michelle Spigner, and Dr. Michelle Wyatt for guidance on developing the research idea. This work is partially funded by the National Institutes of Health (NIH) Grant 1R35GM150565.

REFERENCES

(1) Durand, G. A.; Raoult, D.; Dubourg, G. Antibiotic Discovery: History, Methods and Perspectives. *Int. J. Antimicrob. Agents* **2019**, *53* (4), 371−382.

(2) Lewis, K. The Science of Antibiotic Discovery. *Cell* **2020**, *181* (1), 29−45.

(3) Iskandar, K.; Murugaiyan, J.; Hammoudi Halat, D.; Hage, S. E.; Chibabhai, V.; Adukkadukkam, S.; Roques, C.; Molinier, L.; Salameh, P.; Van Dongen, M. Antibiotic Discovery and Resistance: The Chase and the Race. *Antibiot. Basel Switz.* **2022**, *11* (2), 182.

(4) Epand, R. M.; Walker, C.; Epand, R. F.; Magarvey, N. A. Molecular Mechanisms of Membrane Targeting Antibiotics. *Biochim. Biophys. Acta BBA - Biomembr.* **2016**, *1858* (5), 980−987.

(5) Hurdle, J. G.; O'Neill, A. J.; Chopra, I.; Lee, R. E. Targeting Bacterial Membrane Function: An Underexploited Mechanism for Treating Persistent Infections. *Nat. Rev. Microbiol.* **2011**, *9* (1), 62−75.

(6) Ghosh, C.; Haldar, J. Membrane-Active Small Molecules: Designs Inspired by Antimicrobial Peptides. *ChemMedChem.* **2015**, *10* (10), 1606−1624.

(7) Teixeira, V.; Feio, M. J.; Bastos, M. Role of Lipids in the Interaction of Antimicrobial Peptides with Membranes. *Prog. Lipid Res.* **2012**, *51* (2), 149−177.

(8) Ramírez-Pérez, O.; Cruz-Ramón, V.; Chinchilla-López, P.; Méndez-Sánchez, N. The Role of the Gut Microbiota in Bile Acid Metabolism. *Ann. Hepatol.* **2017**, *16*, s21−s26.

(9) Wu, J.; Yu, T. T.; Kuppusamy, R.; Hassan, M. M.; Alghalayini, A.; Cranfield, C. G.; Willcox, M. D. P.; Black, D. S.; Kumar, N. Cholic Acid-Based Antimicrobial Peptide Mimics as Antibacterial Agents. *Int. J. Mol. Sci.* **2022**, *23* (9), 4623.

(10) Monte, M. J.; Marin, J. J.; Antelo, A.; Vazquez-Tato, J. Bile Acids: Chemistry, Physiology, and Pathophysiology. *World J. Gastroenterol.* **2009**, *15* (7), 804.

(11) Lin, C.; Wang, Y.; Le, M.; Chen, K.-F.; Jia, Y.-G. Recent Progress in Bile Acid-Based Antimicrobials. *Bioconjugate Chem.* **2021**, *32* (3), 395−410.

(12) Epand, R. F.; Savage, P. B.; Epand, R. M. Bacterial Lipid Composition and the Antimicrobial Efficacy of Cationic Steroid Compounds (Ceragenins). *Biochim. Biophys. Acta BBA - Biomembr.* **2007**, *1768* (10), 2500−2509.

(13) Barman, S.; Buzoglu Kurnaz, L.; Yang, X.; Nagarkatti, M.; Nagarkatti, P.; Decho, A. W.; Tang, C. Facially Amphiphilic Bile Acid-Functionalized Antimicrobials: Combating Pathogenic Bacteria, Fungi, and Their Biofilms. *ACS Infect. Dis.* **2023**, *9* (9), 1769−1782.

(14) Buzoglu Kurnaz, L.; Luo, Y.; Yang, X.; Alabresm, A.; Leighton, R.; Kumar, R.; Hwang, J.; Decho, A. W.; Nagarkatti, P.; Nagarkatti, M.; Tang, C. Facial Amphiphilicity Index Correlating Chemical Structures with Antimicrobial Efficacy. *Bioact. Mater.* **2023**, *20*, 519−527.

(15) Craig, M.; Yarrarapu, S. N. S.; Dimri, M. Biochemistry, Cholesterol. In *StatPearls*; StatPearls Publishing: Treasure Island (FL), 2024.
(16) Luchini, A.; Vitiello, G. Mimicking the Mammalian Plasma Membrane: An Overview of Lipid Membrane Models for Biophysical Studies. *Biomimetics* **2021**, *6* (1), 3.
(17) Wang, Y.; Tang, Y.; Zhou, Z.; Ji, E.; Lopez, G. P.; Chi, E. Y.; Schanze, K. S.; Whitten, D. G. Membrane Perturbation Activity of Cationic Phenylene Ethynylene Oligomers and Polymers: Selectivity against Model Bacterial and Mammalian Membranes. *Langmuir* **2010**, *26* (15), 12509−12514.
(18) Ganewatta, M. S.; Chen, Y. P.; Wang, J.; Zhou, J.; Ebalunode, J.; Nagarkatti, M.; Decho, A. W.; Tang, C. Bio-Inspired Resin Acid-Derived Materials as Anti-Bacterial Resistance Agents with Unexpected Activities. *Chem. Sci.* **2014**, *5* (5), 2011.
(19) Arnt, L.; Rennie, J. R.; Linser, S.; Willumeit, R.; Tew, G. N. Membrane Activity of Biomimetic Facially Amphiphilic Antibiotics. *J. Phys. Chem. B* **2006**, *110* (8), 3527−3532.
(20) Lee, M.-T.; Sun, T.-L.; Hung, W.-C.; Huang, H. W. Process of Inducing Pores in Membranes by Melittin. *Proc. Natl. Acad. Sci. U. S. A.* **2013**, *110* (35), 14243−14248.
(21) Chen, X.; Li, B. Analysis of Co-Localized Biosynthetic Gene Clusters Identifies a Membrane-Permeabilizing Natural Product. *J. Nat. Prod.* **2024**, *87* (7), 1694−1703.
(22) Eisenberg, S.; Haimov, E.; Walpole, G. F. W.; Plumb, J.; Kozlov, M. M.; Grinstein, S. Mapping the Electrostatic Profiles of Cellular Membranes. *Mol. Biol. Cell* **2021**, *32* (3), 301−310.

https://doi.org/10.1021/acsomega.4c09804
ACS Omega 2025, 10, 1727−1734